# Electrical Resistivity and Thermoelectric Power of CuAu Alloy*

K. TERAMOTO
*Department of Physics, University of Osaka Prefecture, Sakai, Osaka, Japan*
AND
M. TACHIKI†
*Department of Physics, Universtiy of California, Los Angles, Calfornia*
(Received 31 August 1967)

The temperature dependences of the electrical resistivity and the thermoelectric power of CuAu alloy in the temperature range between 400° and 700°K are investigated on the basis of the theory recently developed by the authors to explain the origin of the long-period superlattice and the phase transitions in the CuAu alloy. The relaxation time of conduction electrons is determined by the scattering due to the lattice vibrations and the disorder arrangements of the Cu and Au atoms. The latter scattering mechanism is most important for explaining the temperature dependence of electrical resistivity. The energy gaps, which appear in CuAu I and CuAu II, modify the electron velocities in the vicinities of these gaps and cause the changes in the transport coefficients. It is found that the energy gaps in the ⟨110⟩ directions are important for explaining the anomalous behavior of the phase dependences of the transport coefficients, especially that of the thermoelectric power.

## 1. INTRODUCTION

THE CuAu alloy has three phases. Below 653°K, Cu atomic layers and the Au atomic layers are alternately stacked along the $c$ axis of a face-centered lattice. This phase is called CuAu I. In the temperature range between 653 and 683°K, the *long-period* superlattice is stable, and this phase is called CuAu II. This structure is constructed by shifting the crystal lattice of CuAu I by $(\frac{1}{2}a,0,\frac{1}{2}c)$ at intervals of five lattice constants along the $b$ axis. In this phase, the crystal lattice has an orthorhombic deformation and lattice modulations commensurate to the long-period ordering of Cu and Au atoms.[1] Above 683°K, this alloy has the disordered phase (CuAu D). The origin of ordering energies and the mechanism of phase transitions have been studied in a preceding paper.[2] (This paper will be cited as Paper I hereafter).

In CuAu I and CuAu II, the conduction electrons are in longer periodic potentials than that of a face-centered lattice. Thus, corresponding to these crystal periodicities, the one-electron energy spectrum has extra energy gaps in the first Brillouin zone of the usual monatomic face-centered lattice, as shown in Fig. 1. In CuAu I, two kinds of energy gaps appear, which are represented by $(0,0,\pm1)$ and $\{110\}$, respectively. In CuAu II, moreover, each of these energy gaps is split into a pair of energy gaps.[3]

As shown by Sato and Toth[4] and by the authors,[2] the energy gaps in the ⟨110⟩ directions are very important for lowering the energy of conduction electrons and stabilizing the long-period superlattice structure of the CuAu alloy. Therefore, studies of the Fermi surface are very much desired. One way of achieving this objective is to investigate the transport properties of this alloy. Recently, measurements of the electrical resistivity $\rho$ and the thermoelectric power $Q$ have been made by Noguchi.[5] The main features of these experimental results are as follows (see Figs. 7 and 10): At each of the transition points, $\rho$ has a positive jump with increasing temperature. In the disordered phase and at temperatures below about 500°K, $\rho$ increases linearly or almost linearly with increasing temperature. On the other hand, $Q$ has a large positive jump at the transition point from CuAu I to CuAu II and a negative jump at the transition point from CuAu II to CuAu D. In CuAu I, $Q$ changes its sign at about 508°K from negative to positive with increasing temperature, and its magnitude is smaller than that of CuAu D. In CuAu II, the sign of $Q$ is positive and the values of $\gamma$ are larger than those of CuAu D.

The object of this paper is to make a theoretical study on the temperature dependences of the electrical resistivity and thermoelectric power of CuAu alloy. The temperature dependences of transport coefficients come from the temperature dependences of the relaxation time, velocity, and density of states of the conduction

* Supported in part by the National Science Foundation and the Office of Naval Research, Contract No. NONR 233 (88).
† On leave from the Department of Physics, Osaka University, Osaka, Japan.
[1] G. Jehanno and P. Perio, J. Phys. Radium **23**, 854 (1962); G. Jehanno and P. Perio, J. Phys. (Paris) **25**, 966 (1964); M. Tachiki, Phys. Rev. **150**, 440 (1966); K. Okamura, H. Iwasaki, and S. Ogawa, J. Phys. Soc. Japan **21**, 1616 (1966).
[2] M. Tachiki and K. Teramoto, J. Phys. Chem. Solids **27**, 335 (1966).
[3] More pairs of energy gaps which split from each of the energy gaps in CuAu I are expected, corresponding to the higher harmonics of Fourier amplitudes of the order parameter in CuAu II. Besides these, energy gaps due to the lattice modulations (Ref. 1) are also expected. However, these energy gaps are very much smaller than the primary ones mentioned above. Thus, these small energy gaps will be neglected. The small contribution of lattice modulations to the primary pairs of energy gaps (Ref. 1) will be also neglected.
[4] H. Sato and R. S. Toth, Phys. Rev. **124**, 1833 (1961); H. Sato and R. S. Toth, Phys. Rev. Letters **8**, 239 (1962).
[5] S. Noguchi, Toyoa Kenkyu Hokoku **17**, 31 (1963). See, also, H. Sato and R. S. Toth, in *Alloying Behavior and Effects in Concentrated Solid Solutions*, edited by T. B. Massalski (Gordon and Breach Science Publishers, Inc., New York, 1965), p. 34.

electrons at the Fermi surface. The relaxation time of the conduction electrons is determined by the scattering of the conduction electrons by the lattice vibrations and the disorder arrangements of Cu and Au atoms. The scattering probability due to the thermal vibrations is proportional to the absolute temperature since the high-temperature approximation can be used in the temperature range we are concerned with. The scattering probability due to the disorder of atomic arrangements is calculated in Sec. 2 A with the use of the values of order parameters obtained in Paper I.[2] The effect of the disorder scattering is more important for the temperature dependence of the electrical resistivity than that of the energy gaps mentioned below.

The extra energy gaps, which appear in CuAu I and CuAu II, cause decreases in the velocities of conduction electrons near these gaps and thus an increase of the electrical resistivity. On the other hand, the thermoelectric power is a quantity related to curvatures of the energy-band spectrum at the Fermi surface. In the vicinities of the energy gaps, even the signs of the curvatures can be changed by the energy gaps. Therefore, the thermoelectric power is expected to be more strongly affected by the energy gaps than the electrical resistivity. The effects of the {110} energy gaps upon the transport coefficients are taken into account in the calculation of various surface integrals over the Fermi surface in Sec. 2 B. The effects due to the (00±1) energy gaps[6] are neglected since these energy gaps cut the inside of the Fermi sea deeply. The modification of the Fermi surface due to these energy gaps is therefore very small. The temperature dependences of the magnitudes of the {110} energy gaps are calculated with the use of the values of order parameters which have been determined in Paper I.

The electrical resistivity is calculated in Sec. 2, and the thermoelectric power in Sec. 3.

## 2. ELECTRICAL RESISTIVITY

If we choose the coordinate axes $(k_X,k_Y,k_Z)$ as shown in Fig. 1, the electrical resistivity for a polycrystal is expressed by

$$\rho=(\tfrac{1}{3}\sum_i \sigma_{ii})^{-1}, \quad (i=X,Y,Z) \tag{1}$$

where $\sigma_{ii}$ is the $ii$ component of the electrical conductivity tensor. $\sigma_{ii}$ is given by the well-known formula

$$\sigma_{ii}=-\frac{2e^2}{(2\pi)^3}\int\frac{\partial f(E_{\mathbf{k}})}{\partial E_{\mathbf{k}}}\int_{E_{\mathbf{k}}=\text{const}}\tau V_i^2 \times|\mathrm{grad}_{\mathbf{k}}E_{\mathbf{k}}|^{-1}dSdE, \tag{2}$$

where $e$ is the electronic charge, $f(E_{\mathbf{k}})$ is the Fermi-Dirac distribution function, $E_{\mathbf{k}}$ is the electron energy with wave number $\mathbf{k}$, $\tau$ is the relaxation time, and $v_i$ is the $i$ component of electron velocity. Here, we assume for simplicity that the quantity $\int\tau v_i^2/|\mathrm{grad}_{\mathbf{k}}E_{\mathbf{k}}|dS$ does not vary rapidly with $E_{\mathbf{k}}$ in the neighborhood of Fermi energy $\zeta$ and that $\tau$ depends only upon $E_{\mathbf{k}}$ .Then, (2) can be written as

$$\sigma_{ii}(\zeta)=[2e^2/(2\pi)^3]\hbar^{-2}J_{ii}(\zeta)\tau(\zeta), \tag{3}$$

where

$$J_{ii}(\zeta)=\int_{\mathrm{FS}}(\partial E_{\mathbf{k}}/\partial k_i)^2|\mathrm{grad}_{\mathbf{k}}E_{\mathbf{k}}|^{-1}dS. \tag{4}$$

The electrical conductivity is influenced not only by a departure from the crystal periodicity (lattice vibrations and disorder of atomic arrangements) through the relaxation time $\tau(\zeta)$, but also by the property of the Fermi surface through the quantities $J_{ii}(\zeta)$ and $\tau(\zeta)$.

In Secs. 2 A and 2 B the quantities $\tau(\zeta)$ and $J_{ii}(\zeta)$ are calculated, respectively, and in Sec. 2 C the result of a numerical calculation of $\rho$ is given and is compared with experiment.

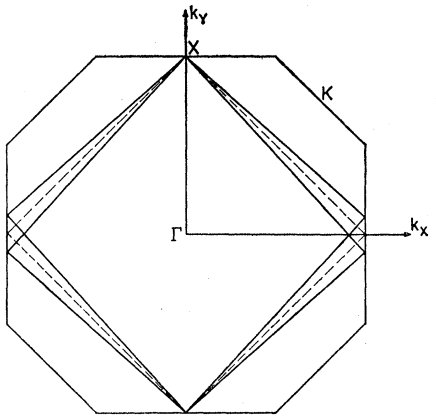


FIG. 1. The (001) cross section of the first Brillouin zone. The dashed lines indicate the energy gaps of CuAu I and the solid lines those of CuAu II.

### A. Calculation of Relaxation Time $\tau(\zeta)$

According to Matthiessen's law, the total scattering probability $1/\tau(\zeta)$ can be written as

$$1/\tau(\zeta)=1/\tau_1(\zeta)+1/\tau_2(\zeta), \tag{5}$$

where $\tau_1(\zeta)$ and $\tau_2(\zeta)$ are the relaxation times due to the thermal vibration of atoms and due to the disorder of atomic arrangements, respectively. The use of this law is considered to be valid in the high-temperature range with which we are concerned .

The scattering probability due to the thermal vibration $1/\tau_1(\zeta)$ is proportional to the absolute temperature since the high-temperature approximation is valid in the temperature range with which we are concerned:

$$1/\tau_1(\zeta)=\gamma(\zeta)T. \tag{6}$$

[6] The {110} or (00±1) energy gaps mean not only the {110} or (00±1) gaps in CuAu I, but also the pairs of gaps, which split from each of them, in CuAu II.

The scattering probability due to the disorder of atomic arrangements $1/\tau_2(\zeta)$ is derived from the usual perturbation theory. The scattering probability $1/\tau_{2i}$, when an electric field is applied in the $i$ $(i=X,Y,Z)$ direction, is given by

$$\frac{1}{\tau_{2i}}=\frac{1}{V}\frac{1}{\frac{1}{4}\hbar\pi^2}\int_{\mathrm{FS}}\langle\langle|V_{\mathbf{k},\mathbf{k}'}|^2\rangle\rangle_T\left(1-\frac{v_i'}{v_i}\right)\frac{dS'}{|\mathrm{grad}_{\mathbf{k}'}E_{\mathbf{k}'}|}, \quad (7)$$

where $V$ is the volume of the crystal, $\langle\langle\ \ \rangle\rangle_T$ means the thermal average, and $V_{\mathbf{k},\mathbf{k}'}$ is the matrix element of the effective perturbing potential $\Delta V(\mathbf{r})$ (which is caused by a departure from the crystal periodicity due to the disorder of atomic arrangements) with respect to the Bloch functions $(1/N)^{1/2}e^{i\mathbf{k}\cdot\mathbf{r}}u_{\mathbf{k}}(\mathbf{r})$ and $(1/N)^{1/2}e^{i\mathbf{k}\cdot\mathbf{r}}u_{\mathbf{k}'}(\mathbf{r})$ of the unperturbed state:

$$V_{\mathbf{k},\mathbf{k}'}=\int(1/N)^{1/2}e^{-i\mathbf{k}\cdot\mathbf{r}}u_{\mathbf{k}}^*(\mathbf{r})\Delta V(\mathbf{r})\times(1/N)^{1/2}e^{i\mathbf{k}'\cdot\mathbf{r}}u_{\mathbf{k}'}(\mathbf{r})d\mathbf{r}. \quad (8)$$

The effective scattering potential $\Delta V(\mathbf{r})$ is constructed in the following way. The ion-core potential, acting on each conduction electron, is expressed by

$$V_c(\mathbf{r})=\sum_{\mathbf{i}}\tfrac{1}{2}[V_{\mathrm{Cu}}(\mathbf{r}-\mathbf{i})(1+\sigma_{\mathbf{i}})+V_{\mathrm{Au}}(\mathbf{r}-\mathbf{i})(1-\sigma_{\mathbf{i}})], \quad (9)$$

where $V_{\mathrm{Cu}}(\mathbf{r})$ and $V_{\mathrm{Au}}(\mathbf{r})$ are the Cu and Au core potentials for conduction electrons and $\sigma_{\mathbf{i}}$ is an order parameter which takes 1 or $-1$ according to whether the lattice site $\mathbf{i}$ is occupied by a Cu atom or an Au atom, respectively. $V_c(\mathbf{r})$ is divided into two parts, the thermal average of $V_c(\mathbf{r})$, $\langle\langle V_c(\mathbf{r})\rangle\rangle_T$, and the deviation from this potential,

$$V_c(\mathbf{r})=\langle\langle V_c(\mathbf{r})\rangle\rangle_T+V_c(\mathbf{r})-\langle\langle V_c(\mathbf{r})\rangle\rangle_T. \quad (10)$$

The first part on the right-hand side of Eq. (10) is included in the unperturbed Hamiltonian, the eigenstates of this Hamiltonian having been obtained in Paper I. The second part is the scattering potential appropriate to the present case, and is written as

$$\Delta V_c(\mathbf{r})=\sum_{\mathbf{i}}v_c(\mathbf{r}-\mathbf{i})(\sigma_{\mathbf{i}}-S_{\mathbf{i}}), \quad (11)$$

where

$$v_c(\mathbf{r}-\mathbf{i})=\tfrac{1}{2}[V_{\mathrm{Cu}}(\mathbf{r}-\mathbf{i})-V_{\mathrm{Au}}(\mathbf{r}-\mathbf{i})], \quad (12)$$

and $S_{\mathbf{i}}$ indicates the thermal average of $\sigma_{\mathbf{i}}$. The potential $v_c(\mathbf{r}-\mathbf{i})$ is expanded in the Fourier series:

$$v_c(\mathbf{r}-\mathbf{i})=\frac{1}{V}\sum_{\mathbf{Q}}v_c(\mathbf{Q})e^{-i\mathbf{Q}\cdot(\mathbf{r}-\mathbf{i})}. \quad (13)$$

This potential is screened by the conduction electrons, and if the dielectric approximation is used, the screened potential is expressed by

$$v_s(\mathbf{r}-\mathbf{i})=\frac{1}{V}\sum_{\mathbf{Q}}\frac{v_c(\mathbf{Q})}{\epsilon(\mathbf{Q})}e^{-i\mathbf{Q}\cdot(\mathbf{r}-\mathbf{i})}, \quad (14)$$

where $\epsilon(\mathbf{Q})$ is the dielectric constant of the conduction electrons for a sinusoidally varying electric field with wave number $\mathbf{Q}$. If Eq. (14) is inserted into Eq. (11) in place of $V_c(\mathbf{r}-\mathbf{i})$, the screened potential of $\Delta V_c(\mathbf{r})$ becomes

$$\Delta V(\mathbf{r})=\sum_{\mathbf{i}}\sum_{\mathbf{Q}}\frac{1}{V}\frac{v_c(\mathbf{Q})}{\epsilon(\mathbf{Q})}e^{-i\mathbf{Q}\cdot(\mathbf{r}-\mathbf{i})}(\sigma_{\mathbf{i}}-S_{\mathbf{i}}). \quad (15)$$

Thus, from Eqs. (8) and (15), $\langle\langle|V_{\mathbf{k},\mathbf{k}'}|^2\rangle\rangle_T$ is calculated as

$$\langle\langle|V_{\mathbf{k},\mathbf{k}'}|^2\rangle\rangle_T=W(\mathbf{h})\left(\frac{1}{N}\right)^2\left[\sum_{\mathbf{K}}\frac{\eta_K(\mathbf{h},\mathbf{k})v_c(\mathbf{K}+\mathbf{h})}{\epsilon(\mathbf{K}+\mathbf{h})}\right]^2, \quad (16)$$

with

$$W(\mathbf{h})=\langle\langle|\sum_{\mathbf{i}}(\sigma_{\mathbf{i}}-S_{\mathbf{i}})e^{i\mathbf{h}\cdot\mathbf{i}}|^2\rangle\rangle_T, \quad (17)$$

$$\eta_{\mathbf{K}}(\mathbf{h},\mathbf{k})=\frac{1}{\Delta}\int_{\Delta}u_{\mathbf{k}}^*(\mathbf{r})u_{\mathbf{k}+\mathbf{h}}(\mathbf{r})e^{-i\mathbf{K}\cdot\mathbf{r}}d\mathbf{r}, \quad (18)$$

and

$$v_c(\mathbf{K}+\mathbf{h})=\int_V\tfrac{1}{2}[V_{\mathrm{Cu}}(\mathbf{r})-V_{\mathrm{Au}}(\mathbf{r})]e^{i(\mathbf{K}+\mathbf{h})\cdot\mathbf{r}}d\mathbf{r}, \quad (19)$$

where $\mathbf{k}$, $\mathbf{h}$, and $\Delta$ are the reciprocal lattice vector, the scattering vector $\mathbf{k}-\mathbf{k}'$, and the volume of the unit cell, respectively.

We rewrite $W(\mathbf{h})$ as

$$W(\mathbf{h})=\sum_{\mathbf{i}}\sum_{\mathbf{i}'}e^{i\mathbf{h}\cdot(\mathbf{i}-\mathbf{i}')}\langle\langle(\sigma_{\mathbf{i}}-S_{\mathbf{i}})(\sigma_{\mathbf{i}'}-S_{\mathbf{i}'})\rangle\rangle_T$$
$$=\sum_{\mathbf{i}}\langle\langle(\sigma_{\mathbf{i}}-S_{\mathbf{i}})^2\rangle\rangle_T+\sum_{\mathbf{i}}\sum_{\mathbf{i}'}e^{i\mathbf{h}\cdot(\mathbf{i}-\mathbf{i}')}\times\langle\langle(\sigma_{\mathbf{i}}-S_{\mathbf{i}})(\sigma_{\mathbf{i}'}-S_{\mathbf{i}'})\rangle\rangle_T, \quad (20)$$

where $i\neq i'$. We neglect for simplicity the second term on the right-hand side of Eq. (20), which expresses the correlation between $\sigma_{\mathbf{i}}-S_{\mathbf{i}}$ and $\sigma_{\mathbf{i}'}-S_{\mathbf{i}'}$ for $\mathbf{i}\neq\mathbf{i}'$. With the use of the Bragg-Williams approximation, the first term of Eq. (2) is calculated as

$$W(\mathbf{h})=\sum_{\mathbf{i}}(1-S_{\mathbf{i}}^2). \quad (21)$$

As shown in Paper I, $S_{\mathbf{i}}$ for CuAu I and CuAu II can be expressed by

$$S_{\mathbf{i}}=S\cos(\mathbf{q}_0,\mathbf{i}), \quad \text{(CuAu I)}$$
$$=\sum_{l=1}^{5}S_{2l-1}\cos(\mathbf{q}_{2l-1},\mathbf{i}), \quad \text{(CuAu II)} \quad (22)$$

with $\mathbf{q}_0=(0,0,2\pi/c)$ and $\mathbf{q}_{2l-1}=(0,(2l-1)\pi/5b,2\pi/c)$.

Substituting Eq. (22) into Eq. (21), we have

$$W(\mathbf{h})=N(1-S^2), \qquad \text{(CuAu I)}$$

$$=N(1-\tfrac{1}{2}\sum_{l=1}^{5} S_{2l-1}{}^2), \quad \text{(CuAu II)}. \qquad (23)$$

Unfortunately, the last part of Eq. (16) is difficult to calculate from first principles, but it seems that this factor does not depend strongly on $\mathbf{h}$. So we assume it to be constant and determine it in the following way. We write the term as

$$\left[\sum_{\mathbf{K}} \frac{\eta_{\mathbf{K}}(\mathbf{h}_1\mathbf{k})v_c(\mathbf{K}+\mathbf{h})}{\epsilon(\mathbf{K}+\mathbf{h})}\right]^2=\frac{\alpha'}{\epsilon}, \qquad (24)$$

where $\alpha'$ and $\epsilon$ are the constants defined by

$$\alpha'=\left[\sum_{\mathbf{K}} \eta_{\mathbf{K}}(\mathbf{h},\mathbf{k})v_c(\mathbf{K}+\mathbf{h})\right]\left[\sum_{\mathbf{K}} \frac{\eta_{\mathbf{K}}(\mathbf{h},\mathbf{k})v_c(\mathbf{K}+\mathbf{h})}{\epsilon(\mathbf{K}+\mathbf{h})}\right], \qquad (25)$$

$$\frac{1}{\epsilon}=\sum \frac{\eta_{\mathbf{K}}(\mathbf{h},\mathbf{k})v_c(\mathbf{K}+\mathbf{h})}{\epsilon(\mathbf{K}+\mathbf{h})} \Big/ \sum \eta_{\mathbf{K}}(\mathbf{h},\mathbf{k})v_c(\mathbf{K}+\mathbf{h}). \qquad (26)$$

$\alpha'$ defined in Eq. (25) has the same form as $\alpha$ in Paper I, but is somewhat different in magnitude because the unperturbed states used here and in Paper I are different. We neglect this small difference and use $\alpha$ in place of $\alpha'$. For the value of $\epsilon$, we tentatively use the value of $\epsilon(q_0)$, which is calculated from the well-known formula

$$\epsilon(\mathbf{q})=1-\frac{4\pi e^2}{Vq^2}\sum_{\mathbf{k}} \frac{f(E_{\mathbf{k}+\mathbf{q}})-f(E_{\mathbf{k}})}{E_{\mathbf{k}+\mathbf{q}}-E_{\mathbf{k}}}. \qquad (27)$$

The summation over $\mathbf{k}$ in Eq. (27) has been performed for several $\mathbf{q}$ including $\mathbf{q}_0$ and $\mathbf{q}_{2l-1}$ by using the energy-band data for copper calculated by Burdick[7] in Paper I.

From Eqs. (16), (23), and (24) we obtain

$$\langle\langle|V_{\mathbf{k},\mathbf{k}'}|^2\rangle\rangle_T=(1/N)(\alpha/\epsilon)(1-S^2), \qquad \text{(CuAu I)}$$

$$=(1/N)(\alpha/\epsilon)(1-\tfrac{1}{2}\sum_{l=1}^{5} S_{2l-1}{}^2). \qquad \text{(CuAu II)}. \qquad (28)$$

Inserting Eq. (28) into Eq. (7) and considering that the second term of Eq. (7) vanishes because of the inversion symmetry of the Fermi surface, we finally obtain for the isotropic scattering probability due to the disorder of atomic arrangements,

$$1/\tau_2(\zeta)=(\pi/\hbar)[N(\zeta)/N](\alpha/\epsilon)(1-S^2), \qquad \text{(CuAu I)}$$

$$=(\pi/\hbar)[N(\zeta)/N](\alpha/\epsilon)(1-\tfrac{1}{2}\sum_{l=1}^{5} S_{2-l1}{}^2), \qquad \text{(CuAu II)}. \qquad (29)$$

[7] G. A. Burdick, Phys. Rev. **129**, 1386 (1963).

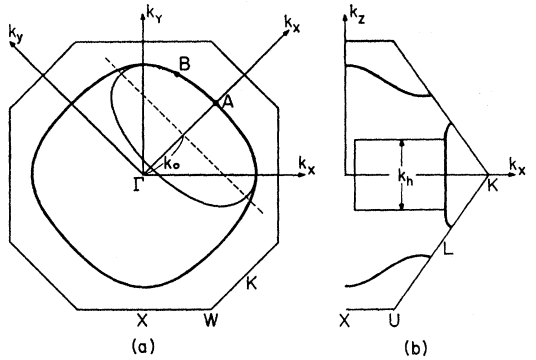


FIG. 2. The Fermi surface of copper obtained by Burdick (see Ref. 7) (thick line) and the elliptical clyinder of height $k_h$ (thin line). (a) (001) cross section, (b) (110) cross section.

$N(\zeta)$ being the density of states at the Fermi surface. We neglect the temperature dependence of $N(\zeta)$[8] and make use of that of copper calculated by Burdick. The temperature dependences of $S$ and $S_{2l-1}$ have been calculated in Paper I.

### B. Calculation of $J_{ii}(\zeta)$

We divide $J_{ii}(\zeta)$ into two parts: $J_{ii}(\zeta)$ of CuAu D, $J_{0ii}(\zeta)$; and the deviation of $J_{ii}(\zeta)$ from $J_{0ii}(\zeta)$, $\Delta J_{ii}(\zeta)$, due to the change in the shape of Fermi surface from that of CuAu D:

$$J_{ii}(\zeta)=J_{0ii}(\zeta)+\Delta J_{ii}(\zeta). \qquad (30)$$

From the cubic symmetry of the crystal, we have the following relation for $J_{0ii}(\zeta)$:

$$J_{0XX}(\zeta)=J_{0YY}(\zeta)=J_{0ZZ}(\zeta)=J_0(\zeta). \qquad (31)$$

Since it is very difficult to calculate $J_0(\zeta)$ by taking into account the conduction-band structure in CuAu D, we leave it as an adjustable parameter.

For the calculation of $\Delta J_{ii}(\zeta)$, we use the energy band of copper calculated by Burdick (see Fig. 2) for that of CuAu D,[9] as we did in the calculation of $H_0(q)$ in Paper I. In the ordered phases, there appear extra energy gaps. Among these energy gaps the {110} energy gaps lying along the flat Fermi surface near the ⟨110⟩ directions contribute most to changing the shape of Fermi surface from that of CuAu D. The (00±1) energy gaps are assumed to affect the shape of Fermi surface only slightly because these gaps cut the inside of the Fermi sea deeply. Therefore, we neglect the contribution to $\Delta J_{ii}(\zeta)$ from the (00±1) energy gaps and take into account only the contributions from the {110} energy gaps.

[8] The deviation of $N(\zeta)$ from $N(\zeta)$ in CuAu D is shown to be proportional to the quantity $\Delta I_{\eta'\eta'}$ defined by Eqs. (82), (83), and (84) in Sec. 3. Since the temperature dependence of $\Delta I_{\eta'\eta'}$ is very small as will be shown in Sec. 3, the temperature dependence of $N(\zeta)$ is very small.

[9] Here the energy-band structure and Fermi surface of CuAu D mean those of a metal having the mean core potential,

$$\tfrac{1}{2}\sum_{\mathbf{i}}[V_{\mathrm{Cu}}(\mathbf{r}-\mathbf{i})+V_{\mathrm{Au}}(\mathbf{r}-\mathbf{i})].$$

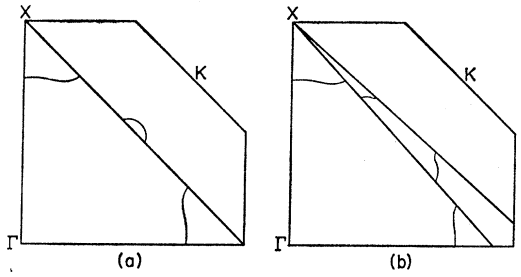


FIG. 3. The (001) cross sections of the Fermi surfaces of CuAu I (a) and CuAu II (b).

As seen from Fig. 1 and Eq. (4), the contributions to $\Delta J_{ii}(\zeta)$ from the Fermi surface in each of the quadrants with respect to the $(k_X,k_Y)$ coordinates are equal to each other in any phase. Therefore, the contribution from the {110} energy gaps is obtained just by multiplying the contribution from the (110) energy gaps by 4.

In order to calculate $\Delta J_{ii}(\zeta)$ due to (110) energy gaps, it is convenient to have an analytical expression of one-electron energy in the vicinity of the Fermi surface of each phase near the [110] direction. As shown in Fig. 2, the Fermi surface of copper near the [110] direction is well expressed by a part of an elliptical cylindrical surface of height $k_h$. Therefore, we approximate the energy expression in the neighborhood of the Fermi surface of CuAu D near [110] direction by

$$E_0(k)=a(k_x-k_0)^2+bk_y^2. \tag{32}$$

The values of $a$ and $k_0$ are determined so that $\partial E_0(k)/\partial k_x$ and $\partial^2 E_0(k)/\partial k_x^2$ at the point $A$ in Fig. 2 coincide with those derived from the energy-band data for copper calculated by Burdick.[7] The value of the Fermi energy $\zeta$ is then given by $E_0(\mathbf{k})$ at the point A. The value of $b$ is determined so that $\zeta=E_0(\mathbf{k})$ passes through the point B in Fig. 2, the cross point bteween the Fermi surface of copper and a line $k_Y=k_X+(\pi/a)$.

We approximate the energy expression of the Fermi surface near a gap in the ordered phases by

$$E(\mathbf{k})=\tfrac{1}{2}\{E_0(\mathbf{k})+E_0(\mathbf{k}-\mathbf{p}) \pm[(E_0(\mathbf{k})-E_0(\mathbf{k}-\mathbf{p}))^2+4U^2]^{1/2}\}, \tag{33}$$

where $2U$ is the magnitude of the energy gap and $\mathbf{p}$ is a vector which indicates the position of the energy gap. Equation (33) is written using Eq. (32) as

$$E(\mathbf{k})=a(k_{x'}^2-p_{x'}k_{x'}+\tfrac{1}{2}p_{x'}^2)+b(k_{y'}-p_{y'}k_{y'}+\tfrac{1}{2}p_{y'}^2) \pm\{[a(-p_{x'}k_{x'}+\tfrac{1}{2}p_{x'}^2) +b(-p_{y'}k_{y'}+\tfrac{1}{2}p_{y'}^2)]^2+U^2\}^{1/2}, \tag{34}$$

where $k_{x'}=k_x-k_0$ and $k_{y'}=k_y$. The values of $p_{x'}$ and $p_{y'}$ are determined so that the energy-gap plane of the energy expression (34) coincides with that[10] derived from the energy-band data calculated by Burdick[7] in the following way. If we indicate the distance from the origin of the $(k_x,k_y)$ coordinates to the energy-gap plane by $l$ and the angle between the energy-gap plane and the $k_y$ axis by $\theta$, the energy-gap plane is represented by

$$(k_{x'}+k_0)\cos\theta+k_{y'}\sin\theta=l. \tag{35}$$

This equation is rewritten as

$$-q_{x'}k_{x'}+\tfrac{1}{2}q_{x'}^2-q_{y'}k_{y'}+\tfrac{1}{2}q_{y'}^2=0, \tag{36}$$

with

$$q_{x'}=2(l-k_0\cos\theta)\cos\theta, \qquad q_{y'}=2(l-k_0\cos\theta)\sin\theta. \tag{37}$$

On the other hand, the energy-gap plane which appears in the energy expression (34) is given by

$$a(-p_{x'}k_{x'}+\tfrac{1}{2}p_{x'}^2)+b(-p_{y'}k_{y'}+\tfrac{1}{2}p_{y'}^2)=0. \tag{38}$$

Comparing Eq. (38) with Eq. (36), we obtain

$$p_{x'}=-\frac{b}{a}\frac{1+\tan^2\theta}{(b/a)+\tan^2\theta}q_{x'}, \qquad p_{y'}=\frac{1+\tan^2\theta}{(b/a)+\tan^2\theta}q_{y'}. \tag{39}$$

The energy gap $2U$ is given by twice the matrix element of the perturbing potential,

$$\tfrac{1}{2}\sum_{\mathbf{i}}[V_{\mathrm{Cu}}(\mathbf{r}-\mathbf{i})-V_{\mathrm{Au}}(\mathbf{r}-\mathbf{i})]S_{\mathbf{i}}, \tag{40}$$

between the Bloch functions $(1/N)^{1/2}u_{\mathbf{k}}(\mathbf{r})e^{i\mathbf{k}\cdot\mathbf{r}}$ and $(1/N)^{1/2}u_{\mathbf{k}-\mathbf{q}}(\mathbf{r})e^{i(\mathbf{k}-\mathbf{q})\cdot\mathbf{r}}$. A calculation similar to that of $V_{\mathbf{k},\mathbf{k}'}$ in Sec. 2a leads to the result

$$U=gS_{\mathbf{q}}\sum_{\mathbf{K}}\eta_{\mathbf{K}}(\mathbf{q},\mathbf{k})v_c(\mathbf{K}+\mathbf{q})/\epsilon(\mathbf{K}+\mathbf{q}), \tag{41}$$

which can be rewritten with the use of $\alpha$ defined in Paper I as

$$U=gS_{\mathbf{q}}\left[\alpha\frac{\sum_{\mathbf{K}}\eta_{\mathbf{K}}(\mathbf{q},\mathbf{k})v_c(\mathbf{K}+\mathbf{q})}{\epsilon(\mathbf{K}+\mathbf{q})}\Big/\sum_{\mathbf{K}}\eta_{\mathbf{K}}(\mathbf{q},\mathbf{k})v_c(\mathbf{K}+\mathbf{q})\right]^{1/2}, \tag{42}$$

where $\eta_{\mathbf{K}}(\mathbf{q},\mathbf{k})$ and $v_c(\mathbf{K}+\mathbf{q})$ are given by Eqs. (18) and (19), respectively, if $\mathbf{h}$ is replaced by $\mathbf{q}$, and $g=1$ for CuAu I and $g=\frac{1}{2}$ for CuAu II. We approximate the second factor in the root of Eq. (42) by $1/\epsilon(\mathbf{q})$, since the terms of $\mathbf{K}=0$ are considered to be dominant both in the denominator and numerator. Thus, from Eqs. (22) and (42), we have $U$ for each phase as

$$U=[\alpha/\epsilon(\mathbf{q}_0)]^{1/2}S, \qquad \text{(CuAu I)} \tag{43}$$

$$U_{2l-1}=\tfrac{1}{2}[\alpha/\epsilon(q_{2l-1})]^{1/2}S_{2l-1}, \qquad \text{(CuAu II)}. \tag{44}$$

[10] Strictly speaking, the position of the each energy gap derived from Burdick's data does not form a plane but a curved surface. It can, however, be replaced by a plane parallel to the $k_z$ axis to a good approximation because it is almost planar. We determined the position of each gap in the plane $k_z=0$.

The values of $\epsilon(\mathbf{q}_0)$ and $\epsilon(\mathbf{q}_{2l-1})$ can be calculated with the use of Eq. (27). As mentioned in the Introduction, we take into account only $U_1$ in CuAu II because the higher harmonics of the Fourier components of the order parameter $S_{2l-1}(l=2\sim5)$ are very small compared with the primary one $S_1$.

The shape of the Fermi surface near the [110] direction in each ordered phase, which is derived from Eqs. (33), (43), and (44), is schematically shown in Fig. 3.

The contribution to $\Delta J_{ii}(\zeta)$ from a (110) energy gap $\Delta\mathcal{J}_{ii}(\zeta)$ can be calculated from

$$\Delta\mathcal{J}_{ii}(\zeta)=\mathcal{J}_{ii}(\zeta)-\mathcal{J}_{0ii}(\zeta), \quad (i=X,Y) \tag{45}$$

with

$$\mathcal{J}_{ii}(\zeta)=k_h\int_{\mathrm{FS}}\left[\frac{\partial E(\mathbf{k})}{\partial k_i}\right]^2|\mathrm{grad}_{\mathbf{k}}E(\mathbf{k})|^{-1}dc, \tag{46}$$

$$\mathcal{J}_{0ii}(\zeta)=k_h\int_{\mathrm{FS}}\left[\frac{\partial E_0(\mathbf{k})}{\partial k_i}\right]^2|\mathrm{grad}_{\mathbf{k}}E_0(\mathbf{k})|^{-1}dc, \tag{47}$$

where $k_h$ is the height of the elliptical cylinder [see Fig. 2(b)]. Here, the integration is taken over the Fermi surface near the energy gap.

If we rewrite Eq. (46) in terms of derivatives with respect to $(k_\xi,k_\eta)$ coordinates (see Fig. 4) defined by

$$\begin{aligned} k_\xi&=k_{x'},\\ k_\eta&=(a/b)^{1/2}k_{y'}, \end{aligned} \tag{48}$$

Eq. (46) becomes

$$\begin{pmatrix}\mathcal{J}_{XX}(\zeta)\\ \mathcal{J}_{YY}(\zeta)\end{pmatrix}=\tfrac{1}{2}k_h\int_{\mathrm{FS}}\left[\begin{pmatrix}a\\ b\end{pmatrix}^{1/2}\left(\frac{\partial E(\mathbf{k})}{\partial k_\xi}\right)^2+\begin{pmatrix}b\\ a\end{pmatrix}^{1/2}\left(\frac{\partial E(\mathbf{k})}{\partial k_\eta}\right)^2 \mp 2\left(\frac{\partial E(\mathbf{k})}{\partial k_\xi}\right)\left(\frac{\partial E(\mathbf{k})}{\partial k_\eta}\right)\right]|\mathrm{grad}_{\mathbf{k}}E(\mathbf{k})|^{-1}dc, \tag{49}$$

with

$$E(\mathbf{k})=a\{k_\xi^2-p_\xi k_\xi+\tfrac{1}{2}p_\xi^2+k_\eta^2-k_\eta p_\eta+\tfrac{1}{2}p_\eta^2 \pm[(-p_\xi k_\xi+\tfrac{1}{2}p_\xi^2-p_\eta k_\eta+\tfrac{1}{2}p_\eta^2)^2+(U/a)^2]^{1/2}\}, \tag{50}$$

where

$$\begin{aligned} p_\xi&=p_{x'},\\ p_\eta&=(b/a)^{1/2}p_{y'}. \end{aligned} \tag{51}$$

We now make another coordinate transformation (see Fig. 4) as

$$\begin{aligned} k_\xi&=k_{\xi'}\cos\phi-k_{\eta'}\sin\phi,\\ k_\eta&=k_{\xi'}\sin\phi+k_{\eta'}\cos\phi, \end{aligned} \tag{52}$$

where $\phi$ is the angle between the energy-gap plane expressed by Eq. (50) and the $k_\eta$ axis, and is given by

$$\cos\phi=[1+(a/b)\tan^2\theta]^{-1/2}. \tag{53}$$

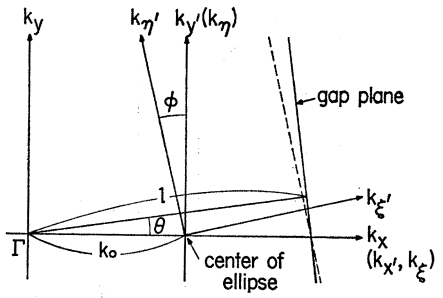


FIG. 4. The coordinate system. The dashed line indicates the energy-gap plane in the $(k_\xi,k_\eta)$ and $(k_{\xi'},k_{\eta'})$ coordinates.

Then, Eq. (49) becomes

$$\begin{pmatrix}\mathcal{J}_{XX}(\zeta)\\ \mathcal{J}_{YY}(\zeta)\end{pmatrix}=\tfrac{1}{2}k_h\{(a/b)^{1/2}(I_{\xi'\xi'}\cos^2\phi+I_{\eta'\eta'}\sin^2\phi -2I_{\xi'\eta'}\sin\phi\cos\phi)+(b/a)^{1/2}(I_{\xi'\xi'}\sin^2\phi+I_{\eta'\eta'}\cos^2\phi +2I_{\xi'\eta'}\sin\phi\cos\phi)\mp2[I_{\xi'\eta'}(\cos^2\phi-\sin^2\phi) +(I_{\xi'\xi'}-I_{\eta'\eta'})\sin\phi\cos\phi]\}, \tag{54}$$

with

$$\begin{aligned} I_{\xi'\xi'}&=\int_{\mathrm{FS}}\left(\frac{\partial E(\mathbf{k})}{\partial k_{\xi'}}\right)^2|\mathrm{grad}_{\mathbf{k}}E(\mathbf{k})|^{-1}dc\\ &=\int_{\mathrm{FS}}\left(\frac{\partial E(\mathbf{k})}{\partial k_{\xi'}}\right)|dk_{\eta'}|,\\ I_{\eta'\eta'}&=\int_{\mathrm{FS}}\left(\frac{\partial E(\mathbf{k})}{\partial k_{\eta'}}\right)^2|\mathrm{grad}_{\mathbf{k}}E(\mathbf{k})|^{-1}dc\\ &=\int_{\mathrm{FS}}\left(\frac{\partial E(\mathbf{k})}{\partial k_{\eta'}}\right)|dk_{\xi'}|,\\ I_{\xi'\eta'}&=\int_{\mathrm{FS}}\left(\frac{\partial E(\mathbf{k})}{\partial k_{\xi'}}\right)\left(\frac{\partial E(\mathbf{k})}{\partial k_{\eta'}}\right)|\mathrm{grad}_{\mathbf{k}}E(\mathbf{k})|^{-1}dc\\ &=\int_{\mathrm{FS}}\left(\frac{\partial E(\mathbf{k})}{\partial k_{\xi'}}\right)\left(\frac{\partial E(\mathbf{k})}{\partial k_{\eta'}}\right)\left|\frac{\partial E(\mathbf{k})}{\partial k_{\xi'}}\right|^{-1}|dk_{\eta'}|, \end{aligned} \tag{55}$$

where

$$E(\mathbf{k})=a\{k_{\xi'}^2-p_{\xi'}k_{\xi'}+\tfrac{1}{2}p_{\eta'}^2+k_{\eta'}^2 +[(-p_{\xi'}k_{\xi'}+\tfrac{1}{2}p_{\xi'}^2)^2+(U/a)^2]^{1/2}\}, \tag{56}$$

$$k_{\xi'}=p_{x'}/\cos\phi. \tag{57}$$

The expressions of $\mathcal{J}_{0ii}(\zeta)$ corresponding to Eqs. (54) and (55) are obtained by replacing $E(\mathbf{k})$ with

$$E_0(\mathbf{k})=a(k_{\xi'}^2+k_{\eta'}^2), \tag{58}$$

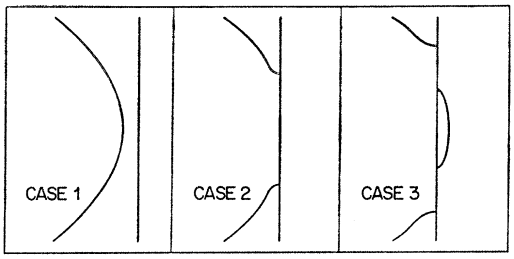


FIG. 5. The three cases of the Fermi surfaces of the energy expression (56). The vertical lines indicate the energy gaps. Case 1: $(\frac{1}{4}ap_{\xi'}{}^2>\zeta+U)$. Case 2: $(\zeta-U<\frac{1}{4}ap_{\xi'}{}^2<\zeta+U)$. Case 3: $(\frac{1}{4}ap_{\xi'}{}^2<\zeta-U)$.

in Eq. (55). Therefore, Eq. (45) becomes

$$\begin{pmatrix}\Delta\mathcal{J}_{XX}(\zeta)\\ \Delta\mathcal{J}_{YY}(\zeta)\end{pmatrix}=\tfrac{1}{2}k_h\{(a/b)^{1/2}(\Delta I_{\xi'\xi'}\cos^2\phi+\Delta I_{\eta'\eta'}\sin^2\phi$$
$$-2\Delta I_{\xi'\eta'}\sin\phi\cos\phi)+(b/a)^{1/2}(\Delta I_{\xi'\xi'}\sin^2\phi$$
$$+\Delta I_{\eta'\eta'}\cos^2\phi+2\Delta I_{\xi'\eta'}\sin\phi\cos\phi)$$
$$\mp 2[\Delta I_{\xi'\eta'}(\cos^2\phi-\sin^2\phi)$$
$$+(\Delta I_{\xi'\xi'}-\Delta I_{\eta'\eta'})\sin\phi\cos\phi]\},\quad(59)$$

with

$$\Delta I_{\xi'\xi'}=I_{\xi'\xi'}-I_{0\xi'\xi'},$$
$$\Delta I_{\eta'\eta'}=I_{\eta'\eta'}-I_{0\eta'\eta'},\quad(60)$$

and

$$\Delta I_{\xi'\eta'}=I_{\xi'\eta'}-I_{0\xi'\eta'},$$

where

$$I_{0\xi'\xi'}=\int_{FS}\left|\frac{\partial E_0(\mathbf{k})}{\partial k_{\xi'}}\right||dk_{\eta'}|,$$
$$I_{0\eta'\eta'}=\int_{FS}\left|\frac{\partial E_0(\mathbf{k})}{\partial k_{q'}}\right||dk_{\xi'}|,\quad(61)$$

and

$$I_{0\xi'\eta'}=\int_{FS}\left[\frac{\partial E_0(\mathbf{k})}{\partial k_{\xi'}}\right]\left[\frac{\partial E_0(\mathbf{k})}{\partial k_{q'}}\right]\left|\frac{\partial E_0(\mathbf{k})}{\partial k_{\xi'}}\right|^{-1}.$$

The integrations over the Fermi surface in Eqs. (55) and (61) are limited only in the neighborhood of the energy gap of $E(\mathbf{k})$. But the contribution to (60) from a region far from the energy gap becomes very small, since the difference in Fermi surface between $E(\mathbf{k})$ and $E_0(\mathbf{k})$ is very small except in the neighborhood of the gap. Therefore, we extend the integration ranges in Eqs. (55) and (61) to those defined by

$$k_{\xi'}\geq\xi_{\min}',$$
$$-\eta_{\max}'\leq k_{\eta'}\leq\eta_{\max}',\quad(62)$$

$\xi_{\min}'$ and $\eta_{\max}'$ being the $k_{\xi'}$ and $k_{\eta'}$ coordinates of the point where $k_{\eta'}$ takes a maximum value on the Fermi surface of $E_0(\mathbf{k})$ or $E(\mathbf{k})$, respectively. From the equations $E_0(\mathbf{k})=\zeta$ and $E(\mathbf{k})=\zeta$, $\xi_{\min}'$ and $\eta_{\max}'$ are obtained as

$$\xi_{\min}'=0,\qquad E_0(\mathbf{k})=\zeta$$
$$=\tfrac{1}{2}p_{\xi'}-[(p_{\xi'})^2-(U/ap_{\xi'})^2]^{1/2}=\xi_m',$$
$$E(\mathbf{k})=\zeta\quad(63)$$

$$\eta_{\max}'=(\zeta/a)^{1/2},\qquad E_0(\mathbf{k})=\zeta$$
$$=[\zeta/a+(U/ap_{\xi'})^2]^{1/2}=\eta_m',\qquad E(\mathbf{k})=\zeta.\quad(64)$$

Thus, with these integration ranges, Eqs. (60) for each of the three cases shown in Fig. 5 become as follows:

Case 1 $(\frac{1}{2}ap_{\xi'}{}^2>\zeta+U)$:

$$\Delta I_{\xi'\xi'}=2\int_0^{\eta_m'}\frac{\partial E_-(\mathbf{k})}{\partial k_{\xi'}}dk_{\eta'}-I_0,$$
$$\Delta I_{\eta'\eta'}=2\int_{\xi_m'}^{\xi_-'}\frac{\partial E_-(\mathbf{k})}{\partial k_{\eta'}}dk_{\xi'}-I_0,\quad(65)$$
$$\Delta I_{\xi'\eta'}=0;$$

Case 2 $(\zeta-U<\frac{1}{2}ap_{\xi'}{}^2<\zeta+U)$:

$$\Delta I_{\xi'\xi'}=2\int_{\eta_+}^{\eta_m'}\frac{\partial E_-(\mathbf{k})}{\partial k_{\xi'}}dk_{\eta'}-I_0,$$
$$\Delta I_{\eta'\eta'}=2\int_{\xi_m'}^{p_{\xi'}/2}\frac{\partial E_-(\mathbf{k})}{\partial k_{\eta'}}dk_{\xi'}-I_0,\quad(66)$$
$$\Delta I_{\xi'\eta'}=0;$$

Case 3 $(\frac{1}{2}ap_{\xi'}{}^2<\zeta-U)$:

$$\Delta I_{\xi'\xi'}=2\int_{\eta_+'}^{\eta_m'}\frac{\partial E_-(\mathbf{k})}{\partial k_{\xi'}}dk_{\eta'}+2\int_0^{\eta_-'}\frac{\partial E_+(\mathbf{k})}{\partial k_{\xi'}}dk_{\eta'}-I_0,$$
$$\Delta I_{\eta'\eta'}=2\int_{\xi_m'}^{p_{\xi'}/2}\frac{\partial E_-(\mathbf{k})}{\partial k_{\eta'}}dk_{\xi'}+2\int_{p_{\xi'}/2}^{\xi_+'}\frac{\partial E_+(\mathbf{k})}{\partial k_{\eta'}}dk_{\xi'}-I_0,\quad(67)$$
$$\Delta I_{\xi'\eta'}=0,$$

where

$$I_0=2\int_0^{(\zeta/a)^{1/2}}\frac{\partial E_0(\mathbf{k})}{\partial k_{\xi'}}dk_{\eta'}$$
$$=2\int_0^{(\zeta/a)^{1/2}}\frac{\partial E_0(\mathbf{k})}{\partial k_{\eta'}}dk_{\xi'}=\pi\zeta,\quad(68)$$

$$\xi_\pm'=\tfrac{1}{2}p_{\xi'}\pm\{\zeta/a+\tfrac{1}{4}p_{\xi'}{}^2-[\zeta p_{\xi'}{}^2/a+(U/a)^2]^{1/2}\}^{1/2},\quad(69)$$

$$\eta_\pm'=(\zeta/a-\tfrac{1}{4}p_{\xi'}{}^2\pm U/a)^{1/2},\quad(70)$$

and

$$E_\pm(k)=a\{k_{\xi'}{}^2-p_{\xi'}k_{\xi'}+\tfrac{1}{2}p_{\xi'}{}^2+k_{\eta'}{}^2$$
$$\pm[(-p_{\xi'}k_{\xi'}+\tfrac{1}{2}p_{\xi'}{}^2)^2+(U/a)^2]^{1/2}\}.\quad(71)$$

Thus, $\Delta J_{ii}(\zeta)$ due to {110} energy gaps is obtained by summing Eq. (59) over the gaps in the first quadrant and multiplying it by 4 as

$$\begin{pmatrix}\Delta J_{XX}(\zeta)\\ \Delta J_{YY}(\zeta)\end{pmatrix}=2k_h\sum_{\text{gap}}[(a/b)^{1/2}(\Delta I_{\xi'\xi'}\cos^2\varphi +\Delta I_{\eta'\eta'}\sin^2\varphi)+(b/a)^{1/2}(\Delta I_{\xi'\xi'}\sin^2\varphi+\Delta I_{\eta'\eta'}\cos^2\varphi) \pm 2(\Delta I_{\xi'\xi'}-\Delta I_{\eta'\eta'})\sin\varphi\cos\varphi], \quad (72)$$

where $\Delta I_{\xi'\xi'}$ and $\Delta I_{\eta'\eta'}$ are given by Eqs. (66) for the outer (110) gap in CuAu II and by Eqs. (67) for the inner (110) gap in CuAu II and for the (110) gap in CuAu I (see Fig. 3).

The results of the numerical calculations of $\Delta J_{XX}(\zeta)$ and $\Delta J_{YY}(\zeta)$ along with $\Delta J(\zeta)=\frac{1}{3}\sum_i \Delta J_{ii}(\zeta)$ are given as functions of temperature in Fig. 6. As seen in this figure, $\Delta J_{ii}(\zeta)$ is negative in both the ordered phases, and its magnitude increases gradually with increasing temperature within each ordered phase. Therefore, the change of the Fermi surface due to the {110} energy gaps gives rise to the increase of resistance, and it has the effect on resistance of making it decrease with increasing temperature, contrary to the case of $(1/\tau(\zeta)$ within each ordered phase. This behavior of $\Delta J_{ii}(\zeta)$ can be understood mainly from the fact that the area of Fermi surface decreases appreciably when there appear {110} gaps just outside the Fermi surface in the ordered phases, and that the smaller the magnitude of each gap becomes with increasing temperature [see Eqs. (43) and (44)], the smaller this effect becomes.

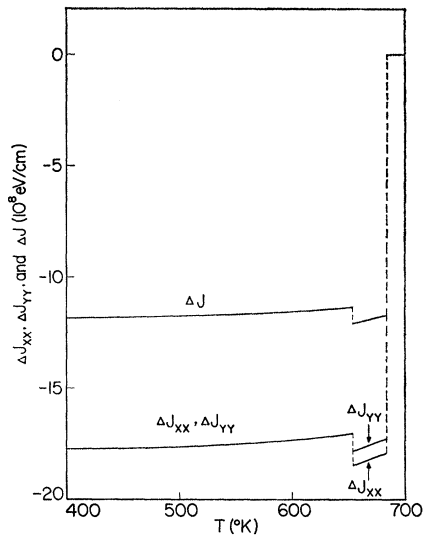


FIG. 6. The temperature dependences of $\Delta J_{XX}(\zeta)$, $\Delta J_{YY}(\zeta)$, and $\Delta J(\zeta)$.

### C. Results and Comparison with Experiments

From Eqs. (1), (3), (5), (30), and (31) we have a somewhat more explicit expression of $\rho$:

$$\rho=[(2\pi)^3\hbar^2/2e^2][\gamma(\zeta)T+1/\tau_2(\zeta)]/[J_0(\zeta)+\Delta J(\zeta)]. \quad (73)$$

The analytic expression of $1/\tau_2(\zeta)$ is given by Eq. (28), and the numerical result of $\Delta J(\zeta)=\frac{1}{3}\sum_i J_{ii}(\zeta)$ is given in Fig. 6. The adjustable parameters $\gamma(\zeta)$ and $J_0(\zeta)$ are determined by the slope of the resistivity-versus-temperature curve obtained experimentally in CuAu D and by the experimental value of resistivity at 683°K, respectively, as

$$\gamma(\zeta)=1.84\times10^{11}\ \text{sec}^{-1}\ \text{deg}^{-1},\quad J_0(\zeta)=5.17\times10^{9}\ \text{eV cm}^{-1}. \quad (74)$$

The temperature dependence of $\rho$ calculated with the use of the values of these parameters is shown in Fig. 7. The calculated values are in good agreement with the experimental values.

In the ordered phases the temperature dependence of $\rho$ is determined almost by the factor $\gamma(\zeta)T+1/\tau_2(\zeta)$ since, as seen from Eq. (74) and Fig. 6, the temperature changes of $J_0(\zeta)+\Delta J(\zeta)$ are very small except at the transition point from CuAu II to CuAu D. Below about 500°K, the crystal of CuAu I is almost perfectly ordered and accordingly $1/\tau_2(\zeta)$ is very small and nearly constant. Therefore, $\rho$ increases nearly linearly with increasing temperature according to $\gamma(\zeta)T$ in that temperature range. On the other hand, $\rho$ increases more rapidly above 500°K in CuAu I than below the temperature, because the order parameter $S$ decreases rapidly as the temperature approaches to the transition point from CuAu I to CuAu II (see Paper I, Fig. 9), and accordingly $1/\tau_2(\zeta)$ increases rapidly with increasing temperature. The degree of order in CuAu II is smaller than that in CuAu I. Thus, at the transition point from CuAu I to CuAu II, $\rho$ has a positive jump by

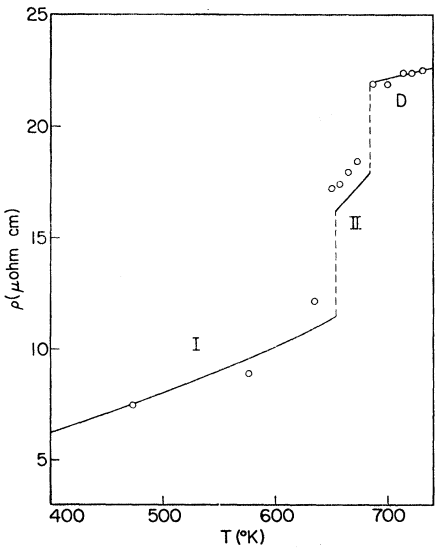


FIG. 7. The temperature dependence of electrical resistivity $\rho$. O indicates the values obtained by Noguchi.

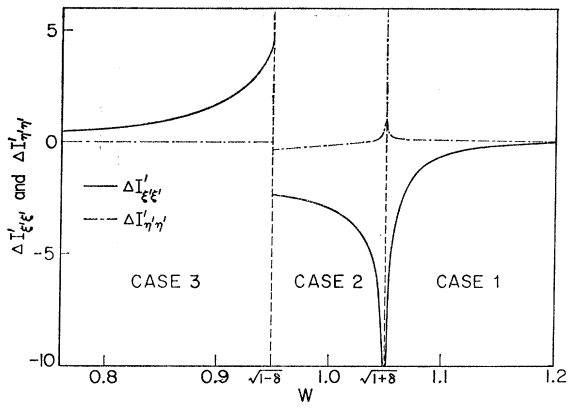


FIG. 8. $\Delta I_{\xi'\xi'}$ and $\Delta I_{\eta'\eta'}$ as functions of $w=\frac{1}{2}(ap_{\xi'}{}^2)^{1/2}$ for $\delta=U/\zeta=0.1$.

the value corresponding to the difference in $1/\tau_2(\zeta)$ between CuAu I and CuAu II.

At 683°K, the crystal of CuAu II makes another phase transition to CuAu D where $1/\tau_2(\zeta)$ becomes largest, and $\Delta J(\zeta)=0$. Although the large change of $1/\tau_2(\zeta)$ at the transition point gives rise to a large positive jump of $\rho$, the change of $\Delta J(\zeta)$ from a large negative value to zero cancels this large positive jump due to $1/\tau_2(\zeta)$ by about half. In CuAu D, $\rho$ increases according to $\gamma(\zeta)T$ since both $1/\tau_2(\zeta)$ and $\Delta J(\zeta)$ are constant.

## 3. THERMOELECTRIC POWER

According to the standard theory,[11] the thermoelectric power due to electron diffusion in a polycrystal is given by

$$Q=\frac{\pi^2k_B{}^2T}{3e}\frac{1}{3}\sum_i\frac{\partial\ln\sigma_{ii}(E)}{\partial E}\bigg|_{E=\zeta},\quad (i=X,Y,Z), \tag{75}$$

where $k_B$ is the Boltzmann constant and $\sigma_{ii}(E)$ is the $ii$ component of the conductivity tensor at absolute zero if the Fermi energy were at $E$, and it is given by Eq. (3) if we assume that $\tau$ depends only upon the electronic energy. The phonon-drag contribution to the thermoelectric power can be neglected since it is negligibly small in the high temperatures we are concerned with.

Substituting Eq. (3) into Eq. (75) and using Eqs. (5), (6), (30), and (31), we have a more explicit expression for $Q$ as

$$Q=\frac{\pi^2k_B{}^2T}{3e}\left[\frac{1}{3}\sum_i\frac{AJ_0(\zeta)+\Delta J_{ii}'(\zeta)}{J_0(\zeta)+\Delta J_{ii}(\zeta)}+B\frac{\gamma(\zeta)T}{\gamma(\zeta)T+1/\tau_2(\zeta)}+C\frac{1/\tau_2(\zeta)}{\gamma(\zeta)T+1/\tau_2(\zeta)}\right], \tag{76}$$

with

$$A=J_0'(\zeta)/J_0(\zeta),\quad B=-\gamma'(\zeta)/\gamma(\zeta),\quad C=-N'(\zeta)/N(\zeta), \tag{77}$$

where primes over $J^0(\zeta)$ etc. mean the derivatives with respect to $E$ at $E=\zeta$. The values of the parameters $J_0(\zeta)$ and $\gamma(\zeta)$ have been determined in Sec. 2 [see Eq. (74)]. The temperature dependences of $1/\tau_2(\zeta)$ and $\Delta J_{ii}(\zeta)$ have been calculated also in Sec. 2 [see Eqs. (29) and (72), and Fig. 6]. The values of $C$ are obtained with the use of the value of $N'(\zeta)$ calculated for copper by the cone model[12,13] as

$$C=0.109\ \text{eV}^{-1}. \tag{78}$$

The quantities $A$ and $B$ are related to the positive thermoelectric power of the noble metals Cu, Ag, and Au. In the case of the pure noble metals, Eq. (76) is reduced to $Q=(\pi^2k_B{}^2T/3e)(A+B)$. Since the electronic charge is a negative quantity, the sign of $A+B$ should be negative for a positive $Q$. Ziman suggested that the contribution to $A$ from the conduction electrons at the {111} necks makes $A$ negative and calculated the value of $A$ using a cone model.[12] But, unfortunately he obtained the result that although $A$ is certainly reduced below the free-electron value $1.5/E_f$, it still remains positive.

On the other hand, Taylor[14] calculated the relaxation time of conduction electrons caused by lattice vibrations taking account of a multiple connection of the Fermi surface of noble metals, and evaluated the value of $B$. Unfortunately he obtained again a positive $B$. After that, Blatt[15] considered the Coulomb scattering of the conduction electrons from the bellies to the necks of the Fermi surface and proposed that the strongly energy-dependent scattering is important for the positive value of $Q$. Therefore, we consider $B$ as including implicitly the contribution from this mechanism. However, since it is very difficult to evaluate the values of $A$ and $B$ from first principles, we consider $A$ and $B$ as adjustable parameters and determine these values by fitting the calculated values of thermoelectric power to the experimental values at the two temperatures 697 and 734°K in the CuAu D phase. The values thus determined are

$$A=-0.139\ \text{eV}^{-1},\quad B=-0.095\ \text{eV}^{-1}. \tag{79}$$

This negative value of $A$ contradicts Ziman's result.

[11] See, for example, J. M. Ziman, *Electrons and Phonons* (Clarendon Press, Oxford, England, 1960), p. 397; D. K. C. MacDonald, *Thermoelectricity* (John Wiley & Sons, Inc., New York, 1962).

[12] J. M. Ziman, Advan. Phys. **10**, 1 (1962).

[13] We determined the energy-gap parameter $u$ in Ref. 13, so that the neck radius coincides with that obtained experimentally and $N(\zeta)$ with that calculated for copper by Burdick (Ref. 7). In the calculation for the value of the effective mass $m^*$, the experimental value of the cyclotron mass of copper at the neck $m_c=0.6m$ [see S. F. Kip, D. N. Langenberg, and W. T. Moore, Phys. Rev. **124**, 359 (1961)] is used since $m^*$ in this model is equal to $m_c$ at the neck.

[14] P. L. Taylor, Proc. Roy. Soc. (London) **A275**, 209 (1963).

[15] F. J. Blatt, Phys. Letters **8**, 235 (1964).

However, it seems that $\Delta$ might be negative, if the actual band structure were used in his calculation.

The next thing we must do is to calculate the values of $\Delta J_{ii}'(\zeta)$. Differentiating Eq. (72) with respect to $\zeta$, we obtain

$$\begin{pmatrix}\Delta J_{XX}'(\zeta)\\ \Delta J_{YY}(\zeta)\end{pmatrix}=2k_h\sum_{\text{gap}}[(a/b)^{1/2}\Delta I_{\xi'\xi'}'\cos^2\phi +\Delta I_{\eta'\eta'}'\sin^2\phi)+(a/b)^{1/2}(\Delta I_{\xi'\xi'}'\sin^2\phi+\Delta I_{\eta'\eta'}'\cos^2\phi) +2(\Delta I_{\xi'\xi'}'-\Delta I_{\eta'\eta'}')\sin\phi\cos\phi], \quad (80)$$

where $\Delta I_{\xi'\xi'}'$ and $\Delta I_{\eta'\eta'}'$ are the derivatives of $\Delta I_{\xi'\xi'}$ and $\Delta I_{\eta'\eta'}$ with respect to $\zeta$, respectively. Taking account of the following relations,

$$\left.\frac{\partial E_\pm(\mathbf{k})}{\partial k_{\xi'}}\right|_{k_{n'}=\eta_\pm'}=0,\quad \left.\frac{\partial E_\pm(\mathbf{k})}{\partial k_{\xi'}}\right|_{k_{n'}=n_{m'}}=0,$$
$$\left.\frac{\partial E_0(\mathbf{k})}{\partial k_{\xi'}}\right|_{k_{\xi'}=\zeta/a}=0,\quad \left.\frac{\partial E_\pm(\mathbf{k})}{\partial k_{\eta'}}\right|_{k_{\xi'}=\xi_\pm'}=0, \quad (81)$$
$$\left.\frac{\partial E_0(\mathbf{k})}{\partial k_{\eta'}}\right|_{k_{\xi'}=\zeta/a}=0,$$

we have the following results for $\Delta I_{\xi'\xi'}'$ and $\Delta I_{\eta'\eta'}'$ from Eqs. (65), (66), and (67).

Case 1:

$$\Delta I_{\xi'\xi'}'=2\hbar\int_0^{\eta_{m'}}\frac{m_{-,\xi'}^{-1}}{v_{-,\xi'}}dk_{\eta'}-\pi,$$
$$\Delta I_{\eta'\eta'}'=2\hbar\int_{\xi_{m'}}^{\xi_-'}\frac{m_{-,\eta'}^{-1}}{v_{-,\eta'}}dk_{\xi'}-\pi; \quad (82)$$

Case 2:

$$\Delta I_{\xi'\xi'}'=2\hbar\int_{\eta_+'}^{\eta_{m'}}\frac{m_{-,\xi'}^{-1}}{v_{-,\xi'}}dk_{\eta'}-\pi,$$
$$\Delta I_{\eta'\eta'}'=2\hbar\int_{\xi_{m'}}^{p\xi'/2}\frac{m_{-,\eta'}^{-1}}{v_{-,\eta'}}dk_{\xi'}-\pi; \quad (83)$$

Case 3:

$$\Delta I_{\xi'\xi'}'=2\hbar\int_{\eta_+'}^{\eta_{m'}}\frac{m_{-,\xi'}^{-1}}{v_{-,\xi'}}dk_{\eta'}+2\hbar\int_0^{\eta_-}\frac{m_{+,\xi'}^{-1}}{v_{+,\xi'}}dk_{\eta'}-\pi,$$
$$\Delta I_{\eta'\eta'}'=2\hbar\int_{\xi_{m'}}^{p\xi'/2}\frac{m_{-,\eta'}^{-1'}}{v_{-,\eta'}}dk_{\xi'}+2\hbar\int_{p\xi'/2}^{\xi_{-1+}}\frac{m_{+,\eta'}}{v_{+,\eta'}}dk_{\xi'}-\pi, \quad (84)$$

where

$$m_{\pm,j}^{-1}=\hbar^{-2}(\partial^2E_\pm(\mathbf{k})/\partial k_j^2), \quad (85)$$
$$v_{\pm,j}=\hbar^{-1}(\partial E_\pm(\mathbf{k})/\partial k_j). \quad (86)$$

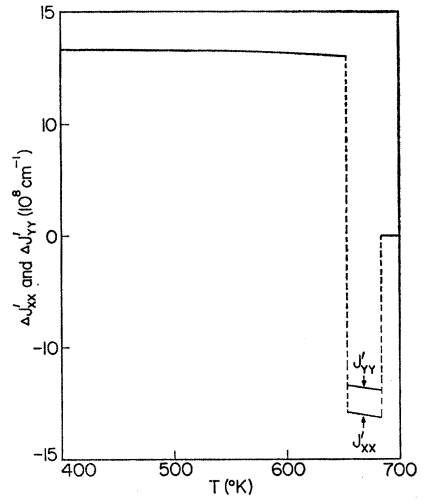


FIG. 9. The temperature dependences of $\Delta J_{XX}'(\zeta)$ and $\Delta J_{YY}'(\zeta)$.

The numerical results of $\Delta I_{\xi'\xi'}'$ and $\Delta I_{\eta'\eta'}'$ for $\delta=U/\zeta=0.1$ are shown in Fig. 8 as functions of $w=(ap_{\xi'}{}^2/4\zeta)^{1/2}$. This figure shows that $\Delta I_{\xi'\xi'}'$ has negative values in case 1 and case 2 and positive values in case 3, and $\Delta I_{\eta'\eta'}'$ has small values in all cases except the boundary between case 1 and case 2. These features of $\Delta I_{\xi'\xi'}'$ and $\Delta I_{\eta'\eta'}'$ are understood from their expressions (82), (83), and(84), and the shape of the Fermi surface shown in Fig. 5 in the following way. On the Fermi surface of the lower branch, the values of $m_{-,\xi'}^{-1}$ are negative near the energy gap, and thus the values of $\Delta I_{\xi'\xi'}'$ for case 1 and case 2 become negative since $v_{-,\xi'}$ is always positive. These negative values are enhanced by the factor $1/v_{-,\xi'}$ because of small values of $v_{-,\xi'}$ near the energy gap. On the Fermi surface of the upper branch, the values of $m_{+,\xi'}^{-1}$ near the energy gap are positive and very much larger compared with those of free electrons. Therefore, the positive contribution to $\Delta I_{\xi'\xi'}'$ from the upper branch, the second term of the first equation of (84), overcomes the negative contribution from the lower branch, the first term of the first equation of (84), and the $\Delta I_{\xi'\xi'}'$ becomes positive in the case 3. On the other hand, $m_{\pm,\eta'}^{-1}$ has exactly the same values as those of free electrons, although the $\eta'$ component of the electron velocity is somewhat affected by the energy gap. Thus, on the whole, we have smaller values of $|\Delta I_{\eta'\eta'}'|$ compared with those of $|\Delta I_{\eta'\eta'}'|$.

The values of $\Delta J_{XX}'(\zeta)$ and $\Delta J_{YY}'(\zeta)$, which are calculated using the values of $\Delta I_{\xi'\xi'}'$ and $\Delta I_{\eta'\eta'}'$ and Eq. (80), are shown in Fig. 9. The positive values of $\Delta J_{XX}'(\zeta)$ and $\Delta J_{YY}'(\zeta)$ are caused by the shape of the Fermi surface near the $\langle 110\rangle$ directions in the each ordered phase as follows. In CuAu I there exist very small number of electrons above the {110} gaps [see Fig. 3(a)]. This corresponds to case 3 and $w$ close to $(1-\delta)^{1/2}$, and thus $\Delta I_{\xi'\xi'}'$ has large positive values and $\Delta I_{\eta'\eta'}'$ has very small negative values as seen in Fig. 8.

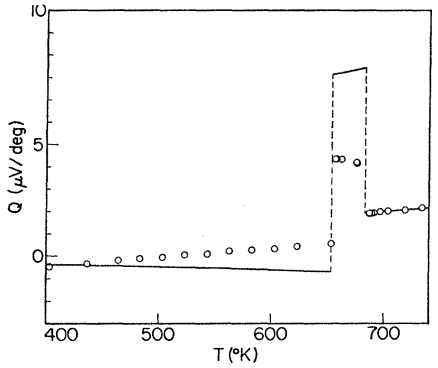


FIG. 10. The temperature dependence of the thermoelectric power $Q$. ○ indicates the values obtained by Noguchi.

Consequently, both the values of $\Delta J_{XX}'(\zeta)$ and $\Delta J_{YY}'(\zeta)$ become positive, since $\phi=0$ in Eq. (80) .

In CuAu II, the outer (110) gap corresponds to case 2 and $w$ close to $(1-\delta)^{1/2}$ [see Fig. 3(b)]. Therefore, $\Delta I_{\xi'\xi'}'$ due to this gap has large negative values, and $\Delta I_{\eta'\eta'}'$ has small negative values. On the other hand,the inner gap corresponds to case 3, and $w$ is far from $(1-\delta)^{1/2}$ [see also Fig. 3(b)]. Therefore, both $\Delta I_{\xi'\xi'}'$ and $\Delta I_{\eta'\eta'}'$ have very small values. Summing up the contribution from the outer and inner gaps, and taking account that $\phi$'s are very small for both gaps, we have negative values for $\Delta J_{XX}'(\zeta)$ and $\Delta J_{YY}'(\zeta)$.

The temperature dependence of $Q$, which is calculated with the use of Eq. (76) and parameters given by Eqs. (74) and (79), is shown in Fig. 10, along with the experimental values obtained by Noguchi. As seen in Fig. 10, $Q$ has a large positive jump at the transition point from CuAu I to CuAu II and somewhat smaller negative jump at the transition point from CuAu II to CuAu I. These behaviors are qualitatively in agreement with the experimental results.

It is seen by comparing Fig. 6 and Fig. 9 with Fig. 10 that the large positive jump at 653°K mainly originates from the negative jump of $\Delta J_{ii}'(\zeta)$, and the negative jump at 683°K from the positive jump of $\Delta J_{ii}(\zeta)$ and $\Delta J_{ii}'(\zeta)$. In fact, the contributions to each jump of $Q$ from the $B$ and $C$ term in Eq. (76) are very small compared with that from the first term in this equation. Consequently, the main features of the phase dependences of $Q$ are ascribed to the structural phase dependences of $\Delta J_{ii}(\zeta)$ and $\Delta J_{ii}(\zeta)'$ due to the change in the shape of the Fermi surface near ⟨110⟩ directions.

Although we can explain the experimental results qualitatively as mentioned above, there are some qualitative discrepancies between the experimental and theoretical values. Firstly, the values of $Q$ in CuAu II are too large and are almost twice the experimental ones. Secondly, the temperature dependence of $Q$ in each of the ordered phases has a trend opposite to that of experiment. We consider the following reasons for the origin of these discrepancies: (1) The structural phase dependences of $B$ and $C$ were neglected in the calculation. However, the value of $B$ and $C$ are expected to vary with structural phase to some extent. (2) The expression (75) is valid under the condition that the integrals

$$\int_{E_k=\text{const}} \tau v_i^2/|\text{grad}_k E_k|\, dS$$

and

$$(E_k-\zeta)\int_{E_k=\text{const}} \tau v_i^2/|\text{grad}_k E_k|\, dS$$

are not violently varying functions of $E_k$ within the energy range of $k_BT$ around the Fermi level. This condition is not completely fulfilled at the higher temperatures in CuAu I where the Fermi energy measured from the bottom of the upper branch is comparable with $k_BT$. Thus, some corrections may be needed in the case of CuAu I.

## ACKNOWLEDGMENTS

The authors would like to express their deepest appreciation to Professor R. Orbach for valuable discussions and for improving the manuscript. One of the authors (K.T.) would like to express his sincere thanks to Professor Y. Kitano for helpful discussions.